JACS
JOURNAL OF THE AMERICAN CHEMICAL SOCIETY

ARTICLE

pubs.acs.org/JACS

Dependence of Avidity on Linker Length for a Bivalent Ligand−Bivalent Receptor Model System

Eric T. Mack, Phillip W. Snyder, Raquel Perez-Castillejos, Başar Bilgiçer, Demetri T. Moustakas, Manish J. Butte, and George M. Whitesides*

Department of Chemistry and Chemical Biology, Harvard University, 12 Oxford Street, Cambridge, Massachusetts 02138, United States

Supporting Information

ABSTRACT: This paper describes a synthetic dimer of carbonic anhydrase, and a series of bivalent sulfonamide ligands with different lengths (25 to 69 Å between the ends of the fully extended ligands), as a model system to use in examining the binding of bivalent antibodies to antigens. Assays based on analytical ultracentrifugation and fluorescence binding indicate that this system forms cyclic, noncovalent complexes with a stoichiometry of one bivalent ligand to one dimer. This dimer binds the series of bivalent ligands with low picomolar avidities ($K_d^{avidity}$ = 3−40 pM). A structurally analogous monovalent ligand binds to one active site of the dimer with K_d^{mono} = 16 nM. The bivalent association is thus significantly stronger ($K_d^{mono}/K_d^{avidity}$ ranging from ∼500 to 5000 unitless) than the monovalent association. We infer from these results, and by comparison of these results to previous studies, that bivalency in antibodies can lead to associations much tighter than monovalent associations (although the observed bivalent association is much weaker than predicted from the simplest level of theory: predicted $K_d^{avidity}$ of ∼0.002 pM and $K_d^{mono}/K_d^{avidity} \sim 8 \times 10^6$ unitless).

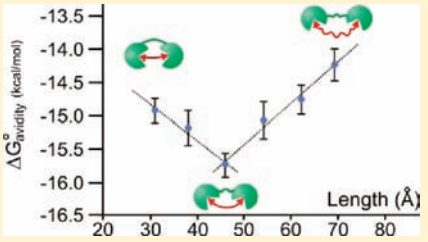

INTRODUCTION

Although antibodies are centrally important components of the immune systems of vertebrates,[1] we understand little about the thermodynamics of these proteins binding to their antigens.[2] We know surprisingly little about the reasons antibodies have the structures they do; in particular, the reasons that the binding regions of all antibodies are dimers (i.e., two Fab domains), or multiples of dimers. Why dimers? Why not a tightly binding monomer? Or a trimer? There is no clear molecular rationale that leads to the conclusion that *two* Fab regions provide the best Darwinian solution to the problems in "molecular defense" posed to the immune system.

In trying to understand why all antibodies have at least two binding sites, we want to understand, quantitatively, the thermodynamics of association between antibodies and their antigens (both monovalent and polyvalent). Understanding the mechanism and thermodynamics that determine the free energy of the association between antibodies and multivalent antigens could, we believe, serve three purposes: (i) it could help to answer the biochemical question of the reason for bi- or oligovalency in antibodies,[3] (ii) it could contribute broadly to understanding oligovalency in molecular biology,[4,5] (iii) it could help in the design of inhibitors of oligovalent interactions, including those involving antibodies.[6,7] In particular, we are interested in the advantage, if any, that bivalency in antibodies affords to the thermodynamics of binding to antigen over that of a monovalent interaction, that of Fab to antigen.

This paper describes a system, a synthetic dimer of carbonic anhydrase (which we call a "dimer of CA", or "$(CA)_2$") and a series of bivalent benzenesulfonamides connected by oligosarcosine linkers (LRL where L is a derivative of benzenesulfonamide) that we use to model the thermodynamics of association between bivalent antibodies and multivalent antigens (Scheme 1). This synthetic dimer of CA is inspired by the structure of immunoglobulins and formed by linking two site-specific mutants of human carbonic anhydrase II (HCAII, EC 4.2.1.1) (Figure 1). We test the influence of the length of the oligosarcosine linker joining the two sulfonamide moieties (LRL) on the strength of the interaction between the synthetic dimer of CA and these sulfonamide ligands.

We recently reported that dimers of CA bound less strongly to ligands immobilized on a surface than would be expected from a simple theory.[3] This theory predicts that the change in free energy ($\Delta G^\circ_{avidity}$) for the bivalent association of $(CA)_2$ to bivalent ligands would be twice the change in enthalpy for the monovalent interaction (ΔH°_{mono}) plus the change in entropy for a single monovalent interaction ($T\Delta S^\circ_{mono}$) (eq 1).[8]

$$\Delta G^\circ_{avidity} = 2\Delta H^\circ_{mono} - T\Delta S^\circ_{mono} \quad (1)$$

In this work, we designed and synthesized a series of bivalent ligands (LRL) with the goal of maximizing the strength of association between LRL and $(CA)_2$. Surprisingly, but also consistent with our previous findings, the strength of association of these ligands to $(CA)_2$ ($\Delta G^\circ_{avidity}$ ranging from −14 to −16 kcal mol^{-1}) is again much less than that predicted

Received: August 5, 2011
Published: November 16, 2011

Scheme 1. Thermodynamic Schemes Describing the Binding of Monovalent Ligands (L) to Monovalent Carbonic Anhydrase CA and Bivalent Benzensulfonamide Ligands (LRL) to a Synthetic Dimer of Carbonic Anhydrase $(CA)_2$[a]

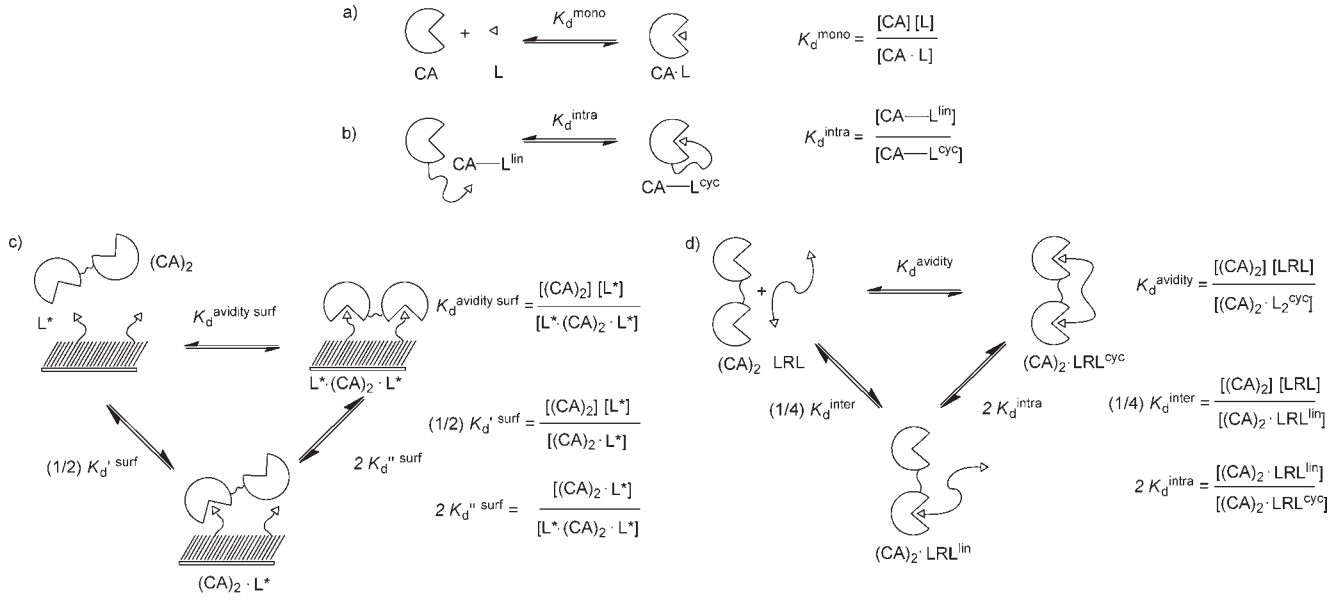

[a] (a) The binding of CA to a monovalent ligand in solution (L) forms a receptor−ligand complex (CA·L) that is characterized by the dissociation constant K_d^{mono}. (b) The binding of a ligand covalently attached to CA by a flexible tether to the binding site is characterized by the unitless dissociation constant K_d^{intra}. (c) The association of $(CA)_2$ to two ligands (L*) on a surface can be conceptualized as a process involving two steps. The initial step, the association of $(CA)_2$ to L*, is characterized by the dissociation constant $K_d'^{surf}$. The second step, the association of an additional ligand to the unbound active site of $(CA)_2$ forms a complex consisting of one $(CA)_2$ and two ligands ($L^*\cdot(CA)_2\cdot L^*$), is characterized by the dissociation constant $K_d''^{surf}$. The avidity ($K_d^{avidity\ surf}$) characterizes the strength of $(CA)_2$ binding to L* in the form of $L^*\cdot(CA)_2\cdot L^*$. (d) The association of a bivalent ligand (LRL) to a dimer of CA (CA_2) can be conceptualized as a process involving two steps. The initial step, the association of one binding moiety of LRL to one binding site of CA_2 to form the "open" complex $(CA)_2\cdot LRL^{lin}$, is characterized by the intermolecular dissociation constant $1/4\ K_d^{inter}$. The second step, the intramolecular association of the unoccupied binding site of $(CA)_2\cdot LRL^{lin}$ to the second binding moiety of LRL to form the cyclic complex $(CA)_2\cdot LRL^{cyc}$, is characterized by the intramolecular dissociation constant $2\ K_d^{intra}$. The overall strength of binding between $(CA)_2$ and LRL is characterized by $K_d^{avidity}$.

by the simplest theory (predicted $\Delta G^\circ_{avidity} = -19$ kcal mol^{-1}). Additionally, we found that varying the length of the linker connecting the arylsulfonamides led only to small, but significant, differences in the free energies of bivalent binding of LRL to $(CA)_2$: the free energies of binding for six bivalent ligands to $(CA)_2$ ($\Delta G^\circ_{avidity}$ ranging from −14 to −16 kcal mol^{-1}) were all within 2 kcal mol^{-1} of each other, despite an end-to-end distance ranging from 31 Å to 69 Å (21 to 41 rotatable bonds).

Schweitzer-Stenner and co-workers quantified the association between monoclonal anti-DNP IgE and a series of bivalent DNP ligands of different lengths (14 Å to 160 Å) using fluorescence titrations.[9] They inferred that the longer ligands (145 Å and 160 Å) were capable of binding bivalently, although weakly, to IgE (enhancements, defined as $K_d^{mono}/K_d^{avidity}$, of 7 to 20 unitless), while the shorter ligands (<132 Å) formed cyclic complexes comprising two antibodies and two ligands with enhancements of 100 to 600. In a series of papers, the Baird group quantified the interaction of antibodies and multivalent ligands often using bivalent DNP ligands, anti-DNP IgE, and cells.[10−12] In one of these studies, Das and co-workers reported the synthesis of a series of bivalent DNP ligands with poly(ethylene glycol) (PEG) linkers (1, 3, and 10 kDa) and characterized their association to monoclonal anti-DNP IgE.[13] They found that cyclic, bivalent complexes can form from the combination of one bivalent ligand and one IgE and observed enhancements of 10 to 300. These results are consistent with those of Schweitzer-Stenner: "long" ligands can bridge the binding sites of a single antibody and form intramolecularly bound, cyclic complexes of one antibody and one L_2. In related work, we characterized the complexes formed from mixtures of monoclonal anti-DNP IgG and a synthetic trivalent DNP ligand.[14] We characterized the stability of these species and found that complexes of two trivalent ligands (L_3) and three antibodies can form in a yield of ∼90% with an enhancement of ∼50.

Bivalent Benzenesulfonamide Ligands LRL and $(CA)_2$ Model Bivalency in Antibodies. We are interested in defining the advantages that bivalent antibodies have over their monovalent counterparts, the Fab domain, both in vivo and in vitro, because we wish to modulate (to inhibit or to enhance) their binding to antigens.[15] We intend the combination of $(CA)_2$ and LRL to serve as a model with which to examine the biophysics and physical−organic chemistry of bivalency in antibodies. This combination of $(CA)_2$ and bivalent sulfonamides is particularly well-suited as a model for bivalent interactions for at least seven reasons: (i) The carbonic anhydrase dimer has the essential structural features of IgG: The dimer consists of two identical binding domains linked by a flexible chain. IgG consists of two identical binding domains linked by two flexible chains to an Fc domain. We can easily change the nature of the linkers (length and flexibility) connecting the binding sites in the dimers.[3] These sorts of changes would require major efforts in mutagenesis to carry out on any IgG. (ii) The carbonic anhydrases (HCA I (28.8 kDa),

dx.doi.org/10.1021/ja2073033 |J. Am. Chem. Soc. 2012, 134, 333–345

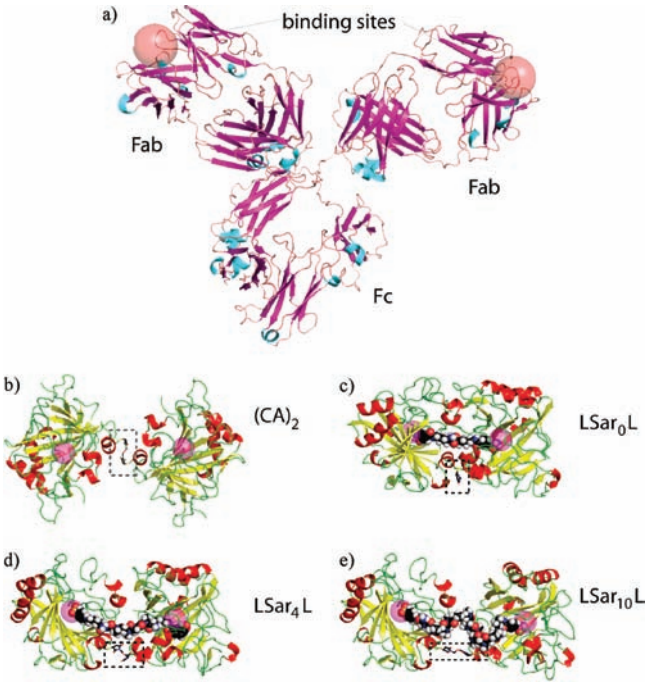

Figure 1. Crystal structures and molecular models of an IgG, and of $(CA)_2$ with and without bivalent ligands. All structures are rendered at the same scale. (a) X-ray crystal structure of a monoclonal murine IgG1 specific for phenolbarbital depicted as a multicolored ribbon diagram (the ribbon diagram was generated using PyMol and the atomic coordinates PDB 1IGY). (b) X-ray crystal structure of (CA_2) with the Zn^{2+} ions of the active site rendered as magenta spheres. The ethylene glycol (EG) cross-linker joining the two monomers of CA is illustrated as atom-colored sticks and outlined with a rectangle with dashed lines (PDB 3PJJ). (c) Molecular model, not an X-ray crystal structure, of $(CA)_2$ with $LSar_0L$ docked in the active sites of $(CA)_2$, to show a possible geometry for a bridging ligand. The bivalent ligand $LSar_0L$ is rendered as atom colored spheres. The structure of the protein is based on the X-ray crystal structure. Details on the construction of the model are included in the Experimental Section. (d) Molecular model of $(CA)_2$ with $LSar_4L$ docked in the active sites. (e) Molecular model of $(CA)_2$ with $LSar_{10}L$ docked in the active sites.

HCA II (29.2 kDa), and bovine carbonic anhydrase BCA II (29.1 kDa), which differ only by 382 Da) are similar in size to the Fabs of IgG (~50 kDa). (iii) HCA is structurally stable and readily available.[16−19] HCA is available in quantities of hundreds of milligrams from *E. coli* with the investment of a few days of work and a minimal cost of supplies. Commercially available monoclonal antibodies (for example, monoclonal anti-DNP antibodies) cost in the range of ~100$ per 0.1 mg. At that cost, conducting a panel of experiments with different ligands, and with enough repeats to provide estimates of uncertainties, would be very expensive (>$10 000). (iv) HCA is easily modified by site-directed mutagenesis. Antibodies are available through site-directed mutagenesis, but their expression from yeast, insect, or mammalian cells is much more challenging and available in fewer academic groups (especially those of physical−organic chemists) than the expression and purification of proteins from *E. coli*. (v) Numerous arylsulfonamides of the general structure R-Ar-SO_2NH_2 bind to HCA in a conserved and well-characterized geometry.[20] The geometry of the sulfonamide ligands in the active site of CA is as well-defined as that of any ligand for any protein; there is no corresponding information on what would happen to a ligand in the binding site of a Fab, if we changed the structure of the ligand.[21] We can think of no monoclonal antibody that has a set of ligands with properties as varied and as well-characterized as the ones that bind to CA. (vi) Synthesis of sulfonamide ligands which bind to CA is tractable, as is their incorporation in bi- and oligovalent systems. (vii) The literature in assays for CA, from enzymatic through fluorescence to surface plasmon resonance and capillary electrophoresis, is much richer for CA than for IgGs. We believe HCA is an excellent model protein, the best we know, for physical−organic studies of protein−ligand binding.[21]

The CAh−Arylsulfonamide Interaction. The carbonic anhydrases bind a wide range of ligands, including arylsulfonamides, with dissociation constants (K_d^{mono}) in the range of micromolar to picomolar.[20,21] The equilibrium for a monovalent ligand (L), a monomeric carbonic anhydrase (CA), and a CA−ligand complex (CA·L) is characterized by the *monovalent* affinity of the interaction, K_d^{mono} (eq 2 and Scheme 1a).

$$K_d^{mono} = \frac{[CA][L]}{[CA\cdot L]} \quad (2)$$

$$\Delta G^\circ_{mono} = RT \ln(K_d^{mono}) \quad (3)$$

Intramolecular Binding of a Tethered Ligand−CA System. In studies aimed at understanding *intramolecular* interactions, we characterized the thermodynamics of binding for the association between the active site of HCA and an arylsulfonamide ligand that was covalently tethered to the surface of HCA by oligo(ethylene glycol) linkers of different lengths (EG_n, n = 0, 2, 5, 10, and 20; Chart 1 and Scheme 1b).[22] We characterized the strength of the intramolecular bond using a unitless dissociation constant K_d^{intra}, the ratio of the concentrations of CA−L^{lin} to CA−L^{cyc} (eq 4, where the en dash represents the covalent attachment between L and CA).

$$K_d^{intra} = \frac{[CA^-L^{lin}]}{[CA^-L^{cyc}]} \quad (4)$$

$$\Delta G^\circ_{intra} = RT \ln(K_d^{intra}) \quad (5)$$

In that system, the relationship between the intramolecular dissociation constant (values of M_{eff} ranging from 0.8 to 26 mM) and the length of the flexible linker (ranging from 25 to 105 Å in extended length between the nitrogen of the sulfonamide and the disulfide bond connecting ligand to the protein) was quantitatively well-explained by a model that describes the linker as a random-coil polymer (eq 6 and Table 1).

$$M_{eff} = K_d^{inter}/K_d^{intra} \quad (6)$$

We inferred from calorimetric studies that the length of the linker influenced the thermodynamics of binding exclusively entropically.[22]

Dimers of CA Bind to Mixed SAMs Presenting Benzenesulfonamides. In studies aimed at understanding the binding of bivalent proteins to ligands on a surface, we developed five synthetic dimers of carbonic anhydrase and studied their interaction with benzenesulfonamide ligands presented at the surface of mixed self-assembled monolayers (SAMs) (Scheme 1c).[3] We prepared three dimers of CA having different lengths of the oligo(ethylene glycol) linker that joined the two molecules of CA, and two dimers with different points of attachment of the linker to the protein. We found that the dimers of CA bound

Chart 1

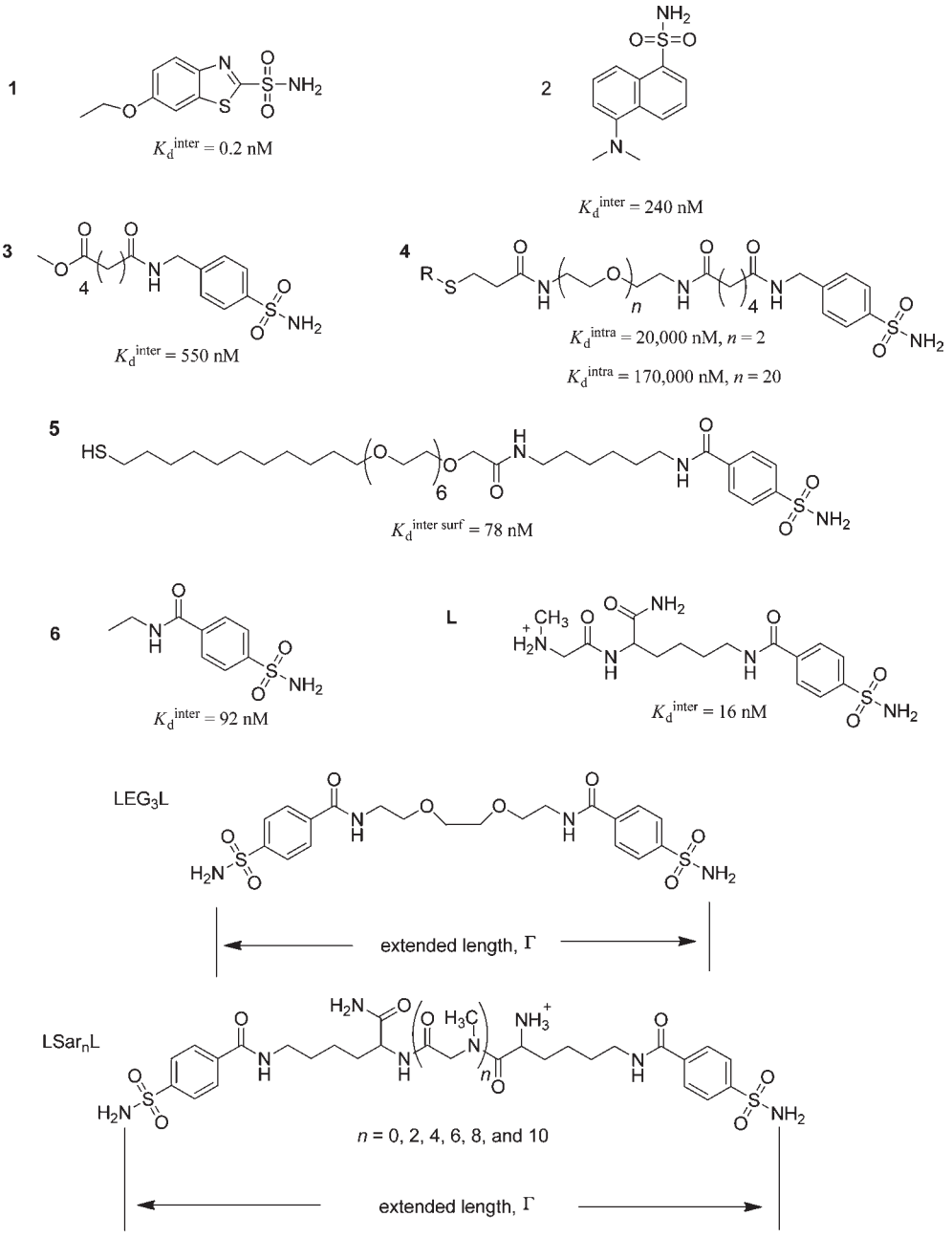

bivalently to the SAM with low nanomolar avidities ($K_d^{avidity\ surf}$ = 1−3 nM, M_{eff} = 3 to 20 μM) while monomeric carbonic anhydrase (CA) bound to the ligands of the SAM less strongly (K_d^{surf} = 89 nM). The bivalent binding of these dimers to the SAM represents a modest ~50-fold enhancement of bivalent over monovalent association. The avidity of these bivalent proteins were unexpectedly insensitive to the structure of the linker connecting them: changing the length of the linker with end-to-end distances between 9 and 18 Å, or the point of attachment between the molecules of CA (either near the active site (C133) or distal to the active site (C185)), had virtually no effect on the avidity of these dimers for the SAM.

Bivalent Interactions in Protein−Ligand Systems. In this paper, we focus on differences in the free energy ($\Delta G°$) of binding of mono- and bivalent ligands to CA, and to a dimer of CA (Scheme 1a and 1d). Scheme 1d diagrams the association of $(CA)_2$ and LRL as a process that involves two steps. Equation 7 (by analogy to eq 3) describes the equilibrium constant for the association of LRL to $(CA)_2$.

$$(1/4)K_d^{inter} = \frac{[(CA)_2][LRL]}{[(CA)_2 \cdot LRL^{lin}]} \quad (7)$$

A dimer of CA is statistically four times more likely to bind a bivalent ligand as monomeric CA is to bind a monovalent ligand because $(CA)_2$ has two binding sites and LRL has two ligand moieties that can bind to CA.[23] The value of K_d^{inter} determines the change in free

dx.doi.org/10.1021/ja2073033 | J. Am. Chem. Soc. 2012, 134, 333–345

Table 1. Dissociation Constants (K_d) and Free Energies ($\Delta G°$) for the Association of Monovalent and Bivalent Ligands to CA and Covalent Dimers of CA, $(CA)_2$'s[a,b]

protein	ligand	$\Delta G°_{mono}$, kcal mol^{-1}	K_d^{mono}, nM	$\Delta G°_{intra}$, kcal mol^{-1}	K_d^{intra}, $\times 10^3$ unitless	$\Delta G°_{avidity}$, kcal mol^{-1}	$K_d^{avidity}$, nM	effective molarity, mM	enhancement, $\times 10^{-3}$ = ($K_d^{mono}/K_d^{avidity}$), $\times 10^{-3}$	ref
HCAII (C206S,K133C)	**1**	−13.2 ± 0.1	0.2	–	–	–	–	–	–	22
HCAII (C206S,K133C)	**2**	−9.10 ± 0.02	230	–	–	–	–	–	–	22
HCAII (C206S,K133C)	**3**	−8.54 ± 0.03	550	–	–	–	–	–	–	22
CA-4 n = 0 to n = 20		–	–	−4.3 to −6.4	0.02 to 0.66	–	–	0.8 to 26	–	22
dimers of CA[c]	**5** surface	−9.1 to −9.7	78 to 200	–	–	11.8 to 12.0	1 to 3	–	0.037 to 0.060	3
HCA II	**6**	−9.6 ± 0.1	92	–	–	–	–	–	–	34
$(CA)_2$	L	−10.6 ± 0.2	16	–	–	–	–	–	–	
$(CA)_2$	LEG_3L	−10.1 ± 0.1	41	–	–	–	–	–	–	
$(CA)_2$	$LSar_0L$	–	–	−3.4 ± 0.2	2.9	−14.9 ± 0.2	0.012	0.005	1.3 ± 0.5	
$(CA)_2$	$LSar_2L$	–	–	−3.7 ± 0.3	1.9	−15.2 ± 0.3	0.008	0.008	2.1 ± 1.0	
$(CA)_2$	$LSar_4L$	–	–	−4.3 ± 0.3	0.7	−15.7 ± 0.3	0.003	0.020	5.3 ± 2.3	
$(CA)_2$	$LSar_6L$	–	–	−3.6 ± 0.3	2.3	−15.1 ± 0.3	0.009	0.007	1.7 ± 0.8	
$(CA)_2$	$LSar_8L$	–	–	−3.3 ± 0.3	3.9	−14.8 ± 0.3	0.015	0.004	1.0 ± 0.5	
$(CA)_2$	$LSar_{10}L$	–	–	−2.7 ± 0.3	9.6	−14.2 ± 0.3	0.038	0.002	0.4 ± 0.2	

[a] This table also contains entries from the literature. [b] Values correspond to the average of three independent experiments. The errors correspond to 90% confidence intervals according to t-statistics. [c] Dimers of CA are a set of proteins that includes $(CA)_2$ and four additional dimers of CA with different linkers.

dx.doi.org/10.1021/ja2073033 | J. Am. Chem. Soc. 2012, 134, 333–345

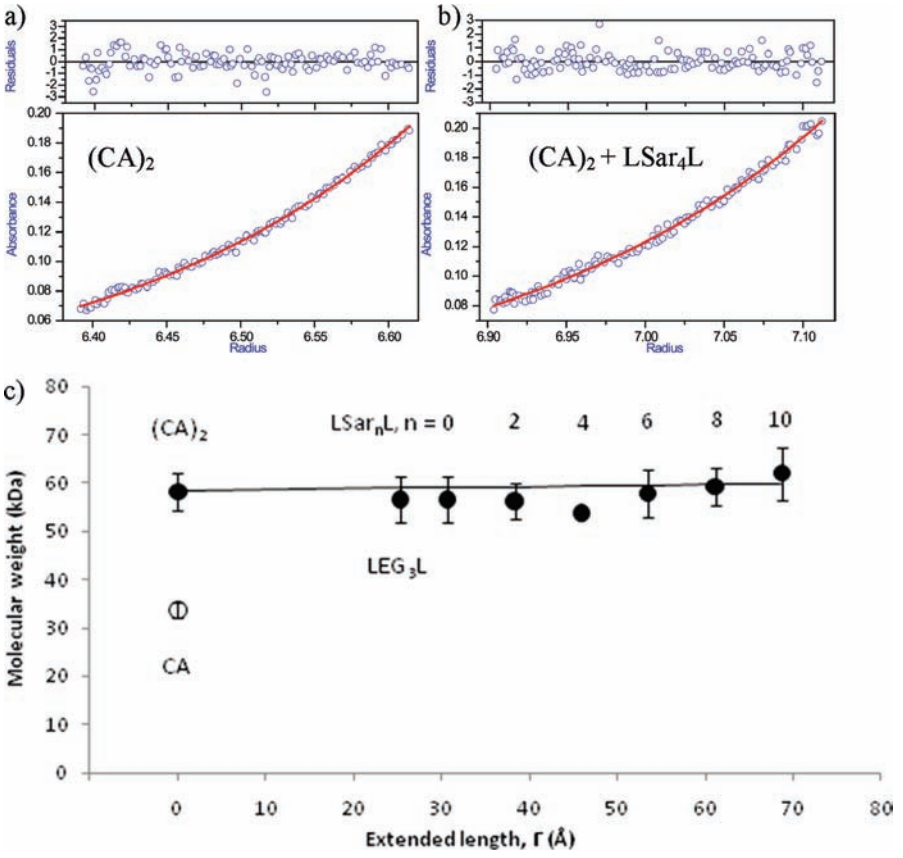

Figure 2. Sedimentation equilibrium experiments of CA and $(CA)_2$ with and without added bivalent ligand as observed at 280 nm and 25 °C. (a) The hollow circles are experimental data for 925 nM $(CA)_2$ without added LRL, and the line is the fit for a single ideal species. The molecular weight estimated by nonlinear curve fitting of the data is 58 ± 4 kDa, and the molecular weight (MW) determined by ESI-MS was 58.385 kDa. (b) The hollow circles are experimental data for 925 nM $(CA)_2$ with 1 μM $LSar_4L$. The molecular weight estimated from nonlinear curve fitting of the data is 54 ± 1 kDa. (c) Plot of the estimated values of MW as determined from sedimentation equilibrium experiments, as a function of the maximum distance between the two nitrogen atoms of the sulfonamide functional groups of the bivalent ligand (Γ is the extended length). The solid circles correspond to the best-fit values for MW calculated from nonlinear curve fitting of the data, and the error bars correspond to the 95% confidence intervals from the nonlinear fit. The solid black line corresponds to the MW obtained from adding the molecular weight of $(CA)_2$ to that of the ligand. These data are summarized in Table S1 and data included in the Supporting Information.

energy for the monovalent binding of $(CA)_2$ to LRL (eq 8).

$$\Delta G^{\circ}_{\text{inter}} = RT \ln(K_d^{\text{inter}}) \quad (8)$$

A dimer of CA can, in principle, form an intramolecular noncovalent bond with a bivalent ligand in which the unoccupied active site of $(CA)_2 \cdot LRL^{lin}$ binds the second sulfonamide of LRL and forms $(CA)_2 \cdot LRL^{cyc}$ (Scheme 1d). At equilibrium, 2 K_d^{intra} equals the concentration of $(CA)_2 \cdot LRL^{lin}$ divided by the concentration of $(CA)_2 \cdot LRL^{cyc}$ (eq 9).[24]

$$2K_d^{\text{intra}} = \frac{[(CA)_2 \cdot LRL^{lin}]}{[(CA)_2 \cdot LRL^{cyc}]} \quad (9)$$

The overall strength of association between $(CA)_2$ and LRL is characterized by the avidity of this bivalent interaction (K_d^{avidity}, M) (eq 10 and Scheme 1d).

$$K_d^{\text{avidity}} = \frac{[(CA)_2][LRL]}{[(CA)_2 \cdot LRL^{cyc}]} = (1/4)K_d^{\text{inter}} \cdot 2K_d^{\text{intra}} \quad (10)$$

It follows from eqs 2 and 5 that the change in free energy for the formation of a cyclic, bivalently bound structure $(CA)_2 \cdot LRL^{cyc}$ ($\Delta G^{\circ}_{\text{avidity}}$) is given by eq 11.

$$\Delta G^{\circ}_{\text{avidity}} = RT \ln(K_d^{\text{avidity}}) \quad (11)$$

The enhancement (β) is the ratio of the monovalent dissociation constant to the avidity and can describe an increase or decrease in the strength of binding between $(CA)_2$ and LRL relative to that of CA and L (eq 12).[15] Values of $\beta > 1$ indicate that $(CA)_2$ binds to LRL more strongly than $(CA)_2$ binds to L.

$$\beta = \frac{K_d^{\text{mono}}}{K_d^{\text{avidity}}} \quad (12)$$

EXPERIMENTAL DESIGN

To characterize the binding of the dimer of CA to the series of bivalent ligands, we estimated values of $\Delta G^{\circ}_{\text{avidity}}$, because comparison of $\Delta G^{\circ}_{\text{avidity}}$ with $\Delta G^{\circ}_{\text{mono}}$ describes the energetic consequence of tethering together two benzenesulfonamides (here, with an oligosarcosine linker). In particular, we wanted to determine the dependence of $\Delta G^{\circ}_{\text{avidity}}$, our metric for the

dx.doi.org/10.1021/ja2073033 |J. Am. Chem. Soc. 2012, 134, 333–345

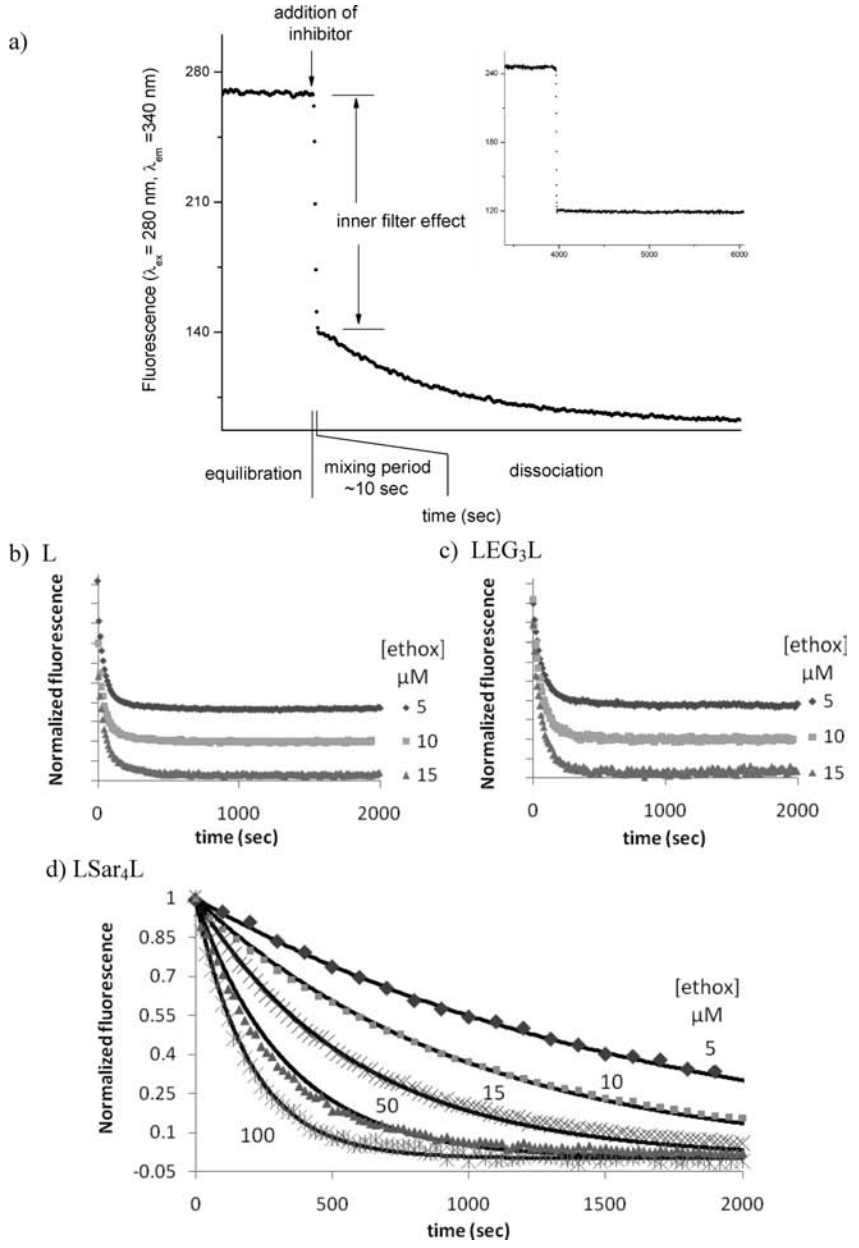

Figure 3. Change in fluorescence (λ_{ex} = 280 nm, λ_{em} = 340 nm) as benzenesulfonamide ligands dissociate from the active sites of $(CA)_2$ (16.7 nM) and are replaced by ethoxzolamide (ethox, K_d = 0.2 nM) which quenches the fluorescence of $(CA)_2$. (a) This plot shows the four steps of kinetic assay: (i) Equilibration of the solution of $(CA)_2$ and ligand in buffer. (ii) Addition of a solution of ethoxzolamide to the stirred solution of $(CA)_2$ is accompanied by a reduction in fluorescence due to the inner filter effect. (iii) The mixing is complete in ~10 s. (iv) The fluorescence decreases as the ligand dissociates from the active sites of $(CA)_2$ and is replaced by ethoxzolamide. Inset: The change in fluorescence as a solution of $(CA)_2$ (16.7 nM) is equilibrated and then a solution of ethoxzolamide (100 nM, K_d = 0.2 nM) is added. (b) Stacked plot of the normalized fluorescence (λ_{ex} = 280 nm, λ_{em} = 340 nm) of a solution of $(CA)_2$ (16.7 nM) and L (160 nM) when ethoxzolamide (5, 10, and 15 μM) is added. These data are corrected for the inner-filter effect and normalized. (c) Stacked plot of the normalized fluorescence of a solution of $(CA)_2$ (16.7 nM) and LEG_3L (160 nM) when ethoxzolamide (5, 10, and 15 μM) is added. (d) Normalized fluorescence of a solution of $(CA)_2$ (16.7 nM) and $LSar_4L$ (160 nM) when ethoxzolamide (6.25, 12.5, 25, 50, and 100 μM) is added. The solid shapes represent the data, and the solid lines are an aid to the eye.

strength of bivalent binding, on the length of the linker joining the two benzenesulfonamides of the ligand.

We synthesized bivalent derivatives of benzenesulfonamides with oligosarcosine linkers with 0, 2, 4, 6, 8, 10 sarcosine units ($LSar_nL$ in Chart 1). We chose oligosarcosines as the linkers because they are typically more soluble in aqueous solutions than other peptides.[25] Oligomers of sarcosine show little nonspecific binding to proteins because the *N*-methyl group prevents hydrogen bonding between the nitrogen of the amide and the carbonyl oxygens of the protein.[26,27] We selected the number of sarcosine units comprising the different linkers (n = 0, 2, 4, 6, 8, 10) to provide lengths (31 to 69 Å) that range from "similar to" to "larger than", the minimum distance required to bridge the active sites of the dimer of CA (~30 Å). We also employed a short bivalent ligand (25 Å) with a tri(ethylene glycol) linker (LEG_3L in Chart 1). We hypothesized that LEG_3L would not bind

dx.doi.org/10.1021/ja2073033 |*J. Am. Chem. Soc.* 2012, 134, 333–345

Scheme 2. Kinetic Scheme Describing the Dissociation of a Bivalent Ligand (LRL) from $(CA)_2$ in the Presence of Ethoxzolamide (◀)

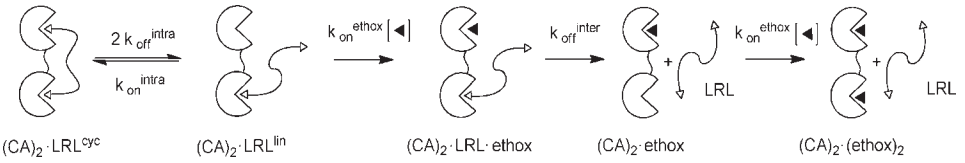

bivalently to the dimer of CA, because this ligand is shorter than the minimum distance between the binding sites of the dimer. We used LEG_3L as a control of monovalent binding to which we compared the longer ligands of $LSar_nL$.

Numerous complexes defined by different stoichiometries, represented by $((CA)_2)_n\cdot(LRL)_m$, can, in principle, form from mixtures of $(CA)_2$ and LRL.[28] The tendency of multivalent systems of receptors and ligands to form complexes of different stoichiometry in the same solution, coupled with the difficulties in determining which complexes are formed, represents a significant barrier in the determination of the free energies of association of multivalent interactions. We conducted two assays (analytical ultracentrifugation (AUC) and a kinetic assay based on observing the dissociation of LRL from $(CA)_2$) that allowed us to determine the stoichiometry of $((CA)_2)_n\cdot(LRL)_m$ complexes. We used this information to construct a mathematical model that we fit to the data from a fluorescence displacement assay, ultimately extracting values of $\Delta G^\circ_{avidity}$ for the series of LRL binding to $(CA)_2$.

Analytical ultracentrifugation (AUC) is a solution technique that provides an estimate of the molecular weights of proteins and their complexes with ligands.[29] We used AUC to estimate the molecular weights of CA, $(CA)_2$, and mixtures of $(CA)_2$ and LRL and inferred from these measurements the coefficient n in $((CA)_2)_n\cdot(LRL)_m$ complexes. We then used the estimate of n to select a set of equations, a mathematical model, to describe the fluorescence displacement assay.

We developed a kinetic assay to follow the rate of dissociation of bivalent ligands from $(CA)_2$ in the presence of the monovalent inhibitor ethoxzolamide, which competes with LRL for the binding sites of $(CA)_2$. This kinetic assay makes it possible to determine the valency of the interaction between $(CA)_2$ and LRL, that is, to determine the presence of intramolecular noncovalent bonds in these complexes. A dependence of the rate of dissociation of LRL from $(CA)_2$ on the concentration of ethoxzolamide corresponds to the presence of intramolecular noncovalent bonds in the $(CA)_2$−LRL complexes, vide infra.

We followed the binding of $(CA)_2$ to bivalent ligands in the presence of the monovalent ligand dansylamide using a fluorescence competition assay. Dansylamide (DNSA) is weakly fluorescent in buffered solution but becomes fluorescent upon binding to CA.[30] The intensity of the fluorescence of the solution is therefore proportional to the concentration of dimers with DNSA bound in their active sites. There are three advantages to this assay over alternative techniques: (i) it is applicable to a wide variety of ligands that bind to the active site of CA, (ii) it is applicable to all isotypes of CA and its mutants, and (iii) it can be described by a mathematical model, i.e., an equation can be used to describe the equilibria and mass balance of the system, and can thus use the data (fluorescence binding isotherms) to provide estimates for the dissociation constants and the free energies.[22] Comparison of free energies of binding of ligands with different lengths of linker to $(CA)_2$ is the focus of this paper.

RESULTS AND DISCUSSION

Synthesis and Characterization of Dimers of CA. We previously described the preparation of the synthetic dimer of human carbonic anhydrase II ($(CA)_2$) from a double mutant of HCAII.[3]

Preparation of Monovalent and Bivalent Sulfonamides. We prepared a series of bivalent benzenesulfonamide ligands (LRL) with oligosarcosine linkers (n = 0, 2, 4, 6, 8, 10 sarcosine units) using standard techniques of solid-phase peptide synthesis, a bivalent ligand with a tri(ethylene glycol) linker, and the monovalent benzenesulfonamide ligand L. We present many of the experimental results as a function of the distance between the two nitrogen atoms of the bivalent ligands when the ligands are in unstrained conformations that maximize this distance. We call this maximum distance the "extended length of the bivalent ligands", or Γ. We calculated Γ from molecular models of ligands using the software package Chem3D Pro by Cambridgesoft.

$(CA)_2$ and LRL Form Complexes Containing Only One $(CA)_2$. Analytical ultracentrifugation (AUC) is a solution technique that provides an estimate for the molecular weights of proteins and their complexes with ligands. AUC is an optical technique based on the absorbance of light by the solution of protein. We required a concentration of $(CA)_2$ (925 nM) that would provide a suitable ratio for the signal-to-noise in the instrument and adjusted the concentration of LRL to maximize ligand-induced oligomerization. Dembo and Goldstein reported that the total concentration of LRL that maximizes the concentration of complexes with two or more $(CA)_2$'s (that is, $[LRL]_{0,max}$) is a function of the total concentration of bivalent receptors, $[R_2]_0$, and the dissociation constant K_d^{inter} (eq 13).[31]

$$[LRL]_{0,max} = \frac{K_d^{inter}}{2} + [(CA)_2]_0 \qquad (13)$$

Substituting 16 nM for K_d^{inter} and 925 nM for $[(CA)_2]_0$ gives 960 nM for the total concentration of LRL ($[LRL]_{0,max}$); this concentration of LRL (~1 μM) is the one we used in these experiments.

We carried out sedimentation equilibrium experiments on a Beckman XL-I ultracentrifuge at rotor speeds of 8000, 10 000, and 12 000 rpm at 25 °C to verify that in mixtures of 925 nM $(CA)_2$ and 1 μM LRL, only complexes containing one molecule of $(CA)_2$ are formed at equilibrium (Figure 2). It is reasonable to assume that under these conditions the ligands are bound to active sites of $(CA)_2$. This procedure yielded an estimated molecular weight of 58 ± 4 kDa for $(CA)_2$ (Table S1, Supporting Information). This result is indistinguishable from the value of 58.385 kDa for $(CA)_2$ determined by mass spectrometry. The results of the AUC experiments support the conclusion that only

dx.doi.org/10.1021/ja2073033 | J. Am. Chem. Soc. 2012, 134, 333–345

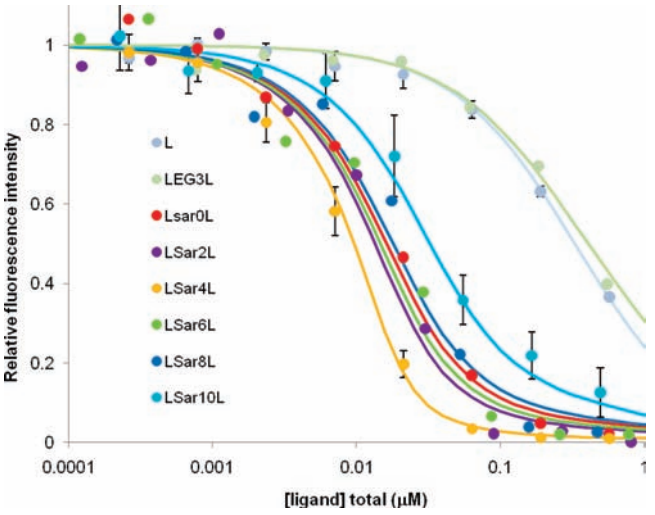

Figure 4. Titration of $(CA)_2$ with monovalent benzenesulfonamide L and bivalent benzenesulfonamide ligands LRL. $(CA)_2$ (25 nM) was equilibrated with 5 μM dansylamide **2** in 20 mM sodium phosphate buffer (pH 7.4) and different amounts of L or LRL. The fluorescence of the solution was monitored with a plate reader (λ_{ex} = 290 nm, λ_{em} = 460 nm). The temperature was maintained at 25 °C. Each datum represents the average of three independent experiments, and the error bars represent the 90% confidence interval according to *t*-statistics. The error bars have been removed from several sets of data for clarity but are similar to those shown. The solid lines represent the best-fit line as determined from nonlinear curve-fitting of eq S21 to each set of data (Supporting Information).

complexes that contain one $(CA)_2$ and one LRL are observed in mixtures of $(CA)_2$ and LRL, when the concentration of $(CA)_2$ is 925 nM or less.

$(CA)_2$ and LRL Dissociate Rapidly in the Presence of High Concentrations of Ethoxzolamide. AUC experiments cannot distinguish between complexes of similar molecular weight; that is, AUC does not tell us if LRL binds to $(CA)_2$ or if a mixture of $(CA)_2\cdot LRL^{lin}$ and $(CA)_2\cdot LRL^{cyc}$ are both present at equilibrium. We require additional structural information on the complexes present at equilibrium to construct the mathematical model that we use to estimate the free energy of association from the fluorescence displacement assay.

We developed a kinetic assay based on fluorescence spectroscopy and confirmed the presence of $(CA)_2\cdot LRL^{cyc}$ by following the rate of dissociation of $LSar_4L$ from $(CA)_2$ in the presence of the soluble monovalent inhibitor, ethoxzolamide, that competes with LRL for the binding sites of $(CA)_2$.[3] This assay consists of four steps (Figure 3a). (i) We allowed a solution of $(CA)_2$ and LRL to equilibrate in a stirred quartz cuvette while the temperature was maintained at 25 ± 1 °C, and we observed the fluorescence of the tryptophan residues of the protein (λ_{ex} = 280 nm, λ_{em} = 340 nm). The benzenesulfonamides of LRL do not quench or enhance the fluorescence of the tryptophan residues when bound to $(CA)_2$. (ii) After the contents of the cuvette reached equilibrium (fluorescence signal did not change with time), we added a solution of ethoxzolamide (K_d^{mono} = 0.2 nM) to the cell. (iii) We observed a decrease in the fluorescence as mixing took place over a period of ~10 s. This initial decrease in fluorescence is a result of the inner-filter effect: the more ethoxzolamide present in the sample the less light that reaches the detector. (iv) During and after the ~10 s mixing period, the fluorescence signal decreases as LRL dissociates from the active sites of $(CA)_2$ and is replaced by ethoxzolamide, which, unlike benzenesulfonamide, quenches the fluorescence of tryptophan residues of CA when bound in the active site.

The rates of dissociation of $LSar_4L$ from $(CA)_2$ increase as the concentration of ethoxzolamide increases (Figure 3d). We infer that $LSar_4L$ binds bivalently to $(CA)_2$. We propose a mechanism consisting of several steps for LRL to dissociate from $(CA)_2$ in the presence of ethoxzolamide (Scheme 2). Ethoxzolamide competes with LRL for the unoccupied binding site of $(CA)_2\cdot LRL^{lin}$. Hence, as the concentration of ethoxzolamide increases, the rate at which ethoxzolamide binds to the unoccupied binding site of $(CA)_2\cdot LRL^{lin}$ (characterized by k_{on}^{ethox} [ethox], Scheme 2) becomes larger than the rate at which the unbound binding moiety of LRL binds to the unoccupied binding site of $(CA)_2\cdot LRL^{lin}$ (characterized by k_{on}^{intra}). The combination of ethoxzolamide with the binding site of $(CA)_2$ is effectively irreversible and increases the rate of dissociation of LRL from $(CA)_2$. When the product ($k_{on}^{ethox}\cdot$[ethox]) is much larger than k_{on}^{intra}, rebinding of $(CA)_2\cdot LRL^{lin}$ to form $(CA)_2\cdot LRL^{cyc}$ is prevented and LRL rapidly dissociates from $(CA)_2$.

We also analyzed the dissociation of L and LEG_3L, which we hypothesized to be too short to span the distance between binding sites of the dimer, from $(CA)_2$ using the same assay. The presence of ethoxzolamide did not affect the rate of dissociation of L and LEG_3L from $(CA)_2$ (Figure 3b and 3c). A rate of dissociation that is independent of the concentration of ethoxzolamide is compatible with a mechanism for dissociation that involves a single dissociation event of the ligand from the active site; in other words, these results indicate that once L dissociates from $(CA)_2$, it does not rebind. On the basis of these results, we included $(CA)_2\cdot LRL^{cyc}$ in the mathematical model that we fit to data from the fluorescent displacement assay to obtain the free energy of bivalent binding in the following section.

Determination of Values of $K_d^{avidity}$ for the Association of LRL's with $(CA)_2$ Using a Fluorescence Displacement Assay. We used a competitive fluorescence-based assay to estimate values of $K_d^{avidity}$ for binding of bivalent sulfonamide ligands to $(CA)_2$ by competition with dansylamide (DNSA; K_d^{mono} ~240 nM) for the active sites of $(CA)_2$ (Figure 4). We began with a concentration of DNSA (5 μM) sufficient to saturate 95% of the active sites of $(CA)_2$ (25 nM), titrated this solution with bivalent ligand (LRL), and followed the disappearance of the fluorescence as the total concentration of LRL increased.

The titration is described by a thermodynamic scheme containing four $(CA)_2$–ligand complexes (i.e., $(CA)_2\cdot(DNSA)_2$, $(CA)_2\cdot LRL\cdot DNSA$, $(CA)_2\cdot LRL^{cyc}$, and $(CA)_2\cdot(LRL)_2$) and three equilibria that connect them (K_1, K_2, and K_3) (Figure 5a). We fit the mathematical description of Figure 5a (eq S21 in Supporting Information) to the titration data using K_d^{intra} as the sole adjustable parameter (Table 1). The Supporting Information details the mathematical description of Figure 5 and the derivation of eq S21. We calculated values of $K_d^{avidity}$ from K_d^{intra} (eq 10) and found that $LSar_4L$ was the tightest binding bivalent ligand (Figure 6).

Values of $\Delta G^\circ_{avidity}$ Lie within a Small Range but Indicate That $LSar_4L$ is the Tightest Binder. The plot of $\Delta G^\circ_{avidity}$ as a function of the extended length shows two trends: the strength of binding increases as Γ increases from 30 to 45 Å, the strength

dx.doi.org/10.1021/ja2073033 |*J. Am. Chem. Soc.* 2012, 134, 333–345

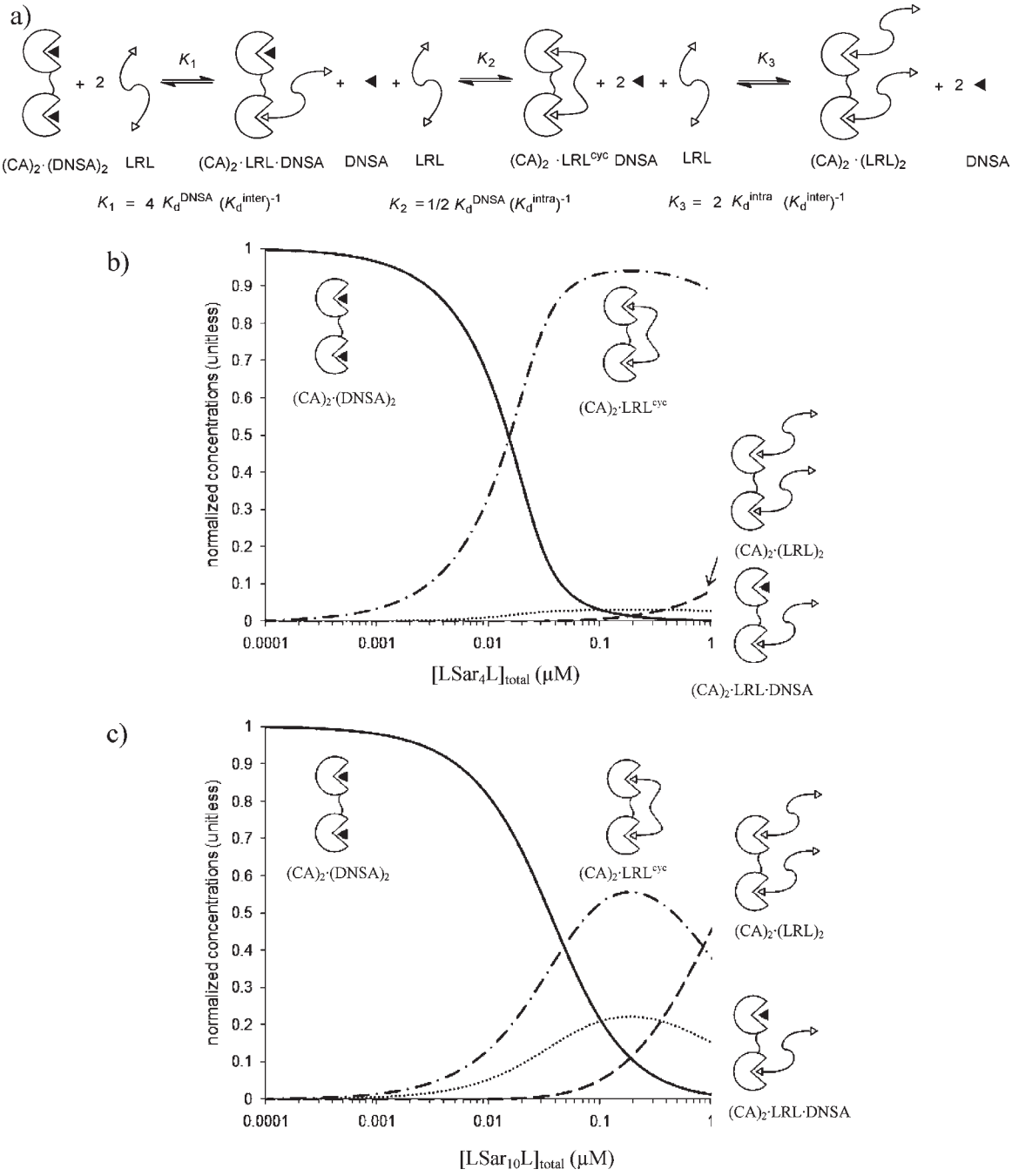

Figure 5. Thermodynamic scheme and simulations describing the model used to analyze the fluorescence titration experiments. (a) The thermodynamic scheme comprises three equilibria characterized by three equilibrium constants (K_1, K_2, and K_3) and four species that contain a dimer of CA (i.e., $(CA)_2 \cdot (DNSA)_2$, $(CA)_2 \cdot LRL \cdot DNSA$, $(CA)_2 \cdot LRL^{cyc}$, and $(CA)_2 \cdot (LRL)_2$). (b) Simulation of the normalized concentrations of species obtained from titrating a solution of $(CA)_2$ (25 nM) and dansylamide (DNSA, 5 μM) with different concentrations of $LSar_4L$ (K_d^{intra} = 0.0007 unitless). The concentration of the cyclic species $(CA)_2 \cdot LRL^{cyc}$ increases until a maximum is reached, as the total concentration of $LSar_4L$ is increased (from left to right). The concentration of $(CA)_2 \cdot LRL^{cyc}$ then decreases as the concentration of unbound $LSar_4L$ is increased, which competes for the active sites of $LSar_4L$. (c) Simulation of the normalized concentrations of species obtained from titrating a solution of $(CA)_2$ (25 nM) and dansylamide (5 μM) with $LSar_{10}L$ (K_d^{intra} = 0.0096 unitless).

reaches a maximum at Γ equal to 45 Å, and then the strength decreases as Γ increases from 45 to 70 Å (Figure 6). Lundquist and Toone have speculated that the length of the linker between the binding moieties of a bivalent ligand should determine the free energy of its interaction with a bivalent protein.[32] In their view, bivalent ligands of less than ideal length can span the distance between two sites of a bivalent receptor but are too short to allow the binding moieties of the bivalent ligand to achieve simultaneously the optimal orientation in the binding sites. They hypothesized that these "short" bivalent ligands will lead to diminished avidity because the sum of the enthalpies of the two interactions will be less than $2\Delta H^{\circ}_{mono}$. Lundquist and

dx.doi.org/10.1021/ja2073033 | J. Am. Chem. Soc. 2012, 134, 333–345

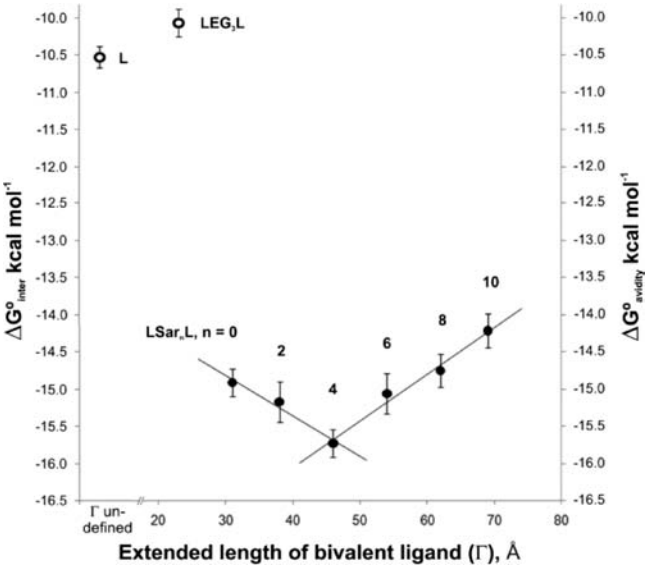

Figure 6. Plot of ΔG°_{inter} and $\Delta G^{\circ}_{avidity}$ for the binding of monovalent (L) and bivalent benzenesulfonamide ligands (LRL) to a synthetic dimer of CA $(CA)_2$ as a function of the extended length of the linker (Γ, Å). The monovalent ligand L does not have an extended length (Γ undefined), but it is included for comparison. The hollow circles are values of ΔG°_{inter} (axis on the left side) and represent the ligands (L and LEG_3L), which do not bind bivalently to $(CA)_2$. The solid circles are values of $\Delta G^{\circ}_{avidity}$ (axis on the right side) and represent the series of bivalent ligands ($LSar_nL$), which bind bivalently to $(CA)_2$. The labels correspond to the number of sarcosines units (n) in the linker. All values are the average of three or more independent experiments, and the errors bars correspond to 90% confidence intervals according to t-statistics.

Toone also suggested that the strength of the bivalent interaction should be at a maximum when the length of the linker is "exactly" the appropriate length (but not longer) to allow both binding moieties of the ligand and both subunits of the receptor to achieve simultaneously optimal orientations. Longer linkers, if the rotatable bonds in the linker are restricted upon the formation of the cyclic complex, diminish the strength of binding because of the unfavorable entropy of restricting rotatable bonds in the linker domain. In our previous work with a covalently tethered system, we found that the free energy of association decreased as the length of the tether connecting ligand to protein increased.[22] The behavior we observe, in this system, for increasing Γ beyond 45 Å is consistent with our previous work. Without characterizing the enthalpic and entropic contributions to binding, however, we cannot evaluate the validity of the model of Lundquist and Toone;[32] although the trends we observe are consistent with their model.

Mixtures of $(CA)_2$ and $LSar_4L$ Form Insoluble Aggregates at Concentrations Needed for Isothermal Titration Calorimetry. We attempted to measure the enthalpy of interaction between LRL and $(CA)_2$ using isothermal titration calorimetry (ITC).[33] We found that precipitates, which we detected as a milky-white suspension following the titration, are formed when $(CA)_2$ (5 μM, required for ITC) is titrated with a solution of LRL (50 μM). We infer from the formation of precipitates that intermolecular binding occurs at these concentrations to form protein–ligand complexes containing more than one $(CA)_2$, although we cannot determine from the formation of precipitates alone the degree to which intermolecular binding competes with the intramolecular binding. Because estimating values of K_d and ΔH° requires a thermodynamic model (e.g., one bivalent ligand binding to one, and only one, bivalent protein), it is impossible to use the data from ITC in this system to determine the enthalpic and entropic contributions to the bivalent interaction. The formation of these precipitates is consistent with the range of effective molarities (2 to 20 μM) we estimated by fluorescence displacement assay; that is, when the total concentration of $(CA)_2$ approaches the value of M_{eff}, intermolecular interactions become increasingly favored over intramolecular interactions.

CONCLUSIONS

$(CA)_2$ Is an Excellent Model for Studying Bivalency in Antibodies. This paper describes a model bivalent receptor inspired by the structure of bivalent antibodies. Dimers of CA are versatile models of bivalency in IgG and IgE because they access a wealth of background information and assays available for CA that are not available for antibodies and because dimers of CA are readily available. This model system allowed us to compare the thermodynamics of binding of bivalent ligands to our previous work with a tethered ligand–CA system[22] and to dimers of CA binding to SAMs.[3] We plan to synthesize dimers of CA, incorporating Fc mimics to explore the role of Fc in the thermodynamics of binding. We believe additional synthetic dimers, in addition to dimers of carbonic anhydrase, can be developed to explore in greater detail the structure–function relationships for antibodies.

$\Delta G^{\circ}_{avidity}$ Is Weaker Than Simple Theory Predicts. The free energy of bivalent binding ($\Delta G^{\circ}_{avidity}$) for the tightest binding bivalent ligand, $LSar_4L$, is much weaker than predicted based on two monovalent interactions of binding. The simplest level of theory predicts that the change in free energy for the bivalent association of $(CA)_2$ to bivalent ligands ($\Delta G^{\circ}_{avidity}$) would be twice the change in enthalpy for the monovalent interaction (ΔH°_{mono}) plus $T\Delta S^{\circ}_{mono}$ for a single monovalent interaction (eq 1).[8] The values of the enthalpy and entropy of binding for monomeric CA to benzenesulfonamide **6** are $\Delta H^{\circ}_{mono} = -9.2$ kcal mol^{-1} and $T\Delta S^{\circ}_{mono} = 0.4$ kcal mol^{-1}.[34] This simple theory estimates a value of $\Delta G^{\circ}_{avidity} = -18.8$ kcal mol^{-1} for $(CA)_2$ and $LSar_4L$, a value that is ~4 kcal mol^{-1} more favorable that the value we observed. The linker could, in principle, influence (favorably or unfavorably) the free energy of the bivalent interaction by interacting with the surface of the protein, although we have established in previous studies that oligomers of sarcosine do not affect the free energy of interaction of arylsulfonamides by associating with the surface of HCA.[26] Unfortunately, we have not been able to obtain a value for the enthalpy for the binding of these ligands to $(CA)_2$ because precipitates are formed at the concentrations required for calorimetry. The thermodynamic basis for the difference between the measured values of $\Delta G^{\circ}_{avidity}$ and those predicted by eq 1, therefore, has not yet been defined.

Variation in $\Delta G^{\circ}_{avidity}$ with the Length of the Linker Is Surprisingly Small. The free energy of the bivalent interaction becomes more favorable as the length of the linker increases until it reaches a minimum at $n = 4$. For ligands with longer linkers, the free energy monotonically increases (i.e., becomes less favorable) with increasing length of the linker.

The values of $\Delta G^{\circ}_{avidity}$ for the bivalent ligands (LRL) differ by less than 2 kcal mol^{-1} between the tightest binding bivalent

ligand ($LSar_4L$) and the weakest binding bivalent ligand ($LSar_{10}L$). The weak dependence of the strength of association on the length of the linker is consistent with our previous studies of intramolecular binding, where variations in oligo(ethylene glycol) linkers from $n = 0$ to 20 resulted in changes of binding of ~2 kcal mol^{-1}. Interestingly, albeit perhaps coincidentally, the variation of the values of $\Delta G^{\circ}_{avidity}$ with increasing length of the sarcosine linker of the ligand is compatible with the thermodynamic analysis of Lundquist and Toone.[32] The length of the linker affects the strength of binding, but length alone cannot account for the ~4 kcal mol^{-1} difference between the value of $\Delta G^{\circ}_{avidity}$ predicted by theory (−19 kcal mol^{-1}) and the values of $\Delta G^{\circ}_{avidity}$ we measured (−15 kcal mol^{-1}).

Tight-Binding Multivalent Ligands Can Be Synthesized with "Long", Flexible Linkers. Consistent with our previous work and the work of others, the results of this paper suggest that flexible bivalent ligands that are longer than the spacing between the binding sites of the receptors can still bind tightly to multivalent proteins.[35] A bivalent ligand ($LSar_4L$) with a linker of "optimal" length, in this system, gave ~2 kcal mol^{-1} more favorable free energy than a bivalent ligand 25 Å longer. The effort required to "optimize" the length of the linker may not be worth the effort to obtain an increase in the strength of binding of ~2 kcal mol^{-1}.

EXPERIMENTAL SECTION

General Methods. Chemicals we purchased from Aldrich, Alfa Aesar, and Novabiochem. NMR experiments were carried out on a Varian INOVA 500 MHz spectometer. Isothermal titration calorimetry (ITC) was performed using a VP-ITC microcalorimeter (MicroCal). UV−vis spectroscopy was conducted on a Hewlett-Packard 8453 spectrophotometer. Analytical HPLC was run on a Varian instrument with a C18 column, 5 μm (4.6 × 250 mm), from Vydac using a linear gradient of water with 0.1% TFA (A) followed by acetonitrile containing 0.08% TFA (B), at a flow rate of 1 mL min^{-1} (UV detection at 218 and 280 nm). Preparative reverse-phase HPLC was performed using a Varian HPLC instrument equipped with a C18 column, 5 μm (22 × 250 mm), from Vydac at a flow rate of 15 mL min^{-1} with UV detection at 218 and 280 nm. Fluorescence measurements were performed on a Perkin-Elmer LS 50 B fluorimeter (kinetic assay) and on a Molecular Devices SpectraMax Gemini XS instrument for detection at 460 nm (for DNSA binding assays).

Synthesis of Monovalent and Bivalent Sulfonamides. All ligands, except LEG_3L, were synthesized using standard Fmoc chemistry by stepwise solid-phase methodology, according to published procedures.[36] The crude mixtures containing ligands were purified by preparative reverse-phase HPLC and the appropriate fractions lyophilized. Purity and molecular weight were consistent with the proposed structure as assessed by analytical RP-HPLC and ESI-HRMS. L: ESI-HRMS m/z found 400.1655 Da; calcd 400.1672 Da. LEG_3L: ESI-HRMS m/z found 537.1115 Da; calcd 537.1090 Da. $LSar_0L$: ESI-HRMS m/z found 640.2209 Da; calcd 640.2223. $LSar_2L$: ESI-HRMS m/z found 782.2980 Da; calcd 782.2966 Da. $LSar_4L$: ESI-HRMS m/z found 924.3718 Da; calcd 924.3708 Da. $LSar_6L$: ESI-HRMS m/z found 1066.44 Da; calcd 1066.44 Da. $LSar_8L$: ESI-HRMS m/z found 1208.52 Da; calcd 1208.52 Da. $LSar_{10}L$: ESI-HRMS m/z found 1350.59 Da; calcd 1350.59 Da.

Quantitation of Stock Solutions of Arylsulfonamide Ligands. Solutions were prepared to ~20 mM by weighing the solid bivalent ligand and then adding the appropriate amount of DMSO-d_6. Stock solutions were diluted 1:10 with 2.00 mM maleic acid standard in DMSO-d_6, which were prepared gravimetrically. Proton resonances from the arylsulfonamide were normalized relative to those from maleic acid (allowing a 10 s delay between pulses) to determine the concentration of the stock solutions accurately.

Analytical Ultracentrifugation (AUC). The molecular weight of $(CA)_2$ with and without added LRL in solution was estimated by sedimentation equilibrium on a Beckman XL-I ultracentrifuge. Concentrations of $(CA)_2$ were fixed at 0.925 μM. Samples were dissolved in 10 mM phosphate buffer (pH 7.40), containing 137 mM NaCl and 2.7 mM KCl. The samples were centrifuged at 6000, 9000, and 12 000 rpm for 22 h at 25 °C before absorbance scans were performed. Data obtained at 25 °C were fit globally to an equation that describes the sedimentation of a homogeneous species using XL-A/XL-I Data Analysis software version 6.03 based on Origin software by OriginLab Software Inc.

Kinetic Assay. A solution of $(CA)_2$ (16.7 nM) and bivalent ligand (160 nM) was prepared in 20 mM PBS (pH 7.4) and centrifuged to remove traces of dust. A 2 mL portion of solution was transferred to a quartz cuvette and the cuvette placed in a Perkin-Elmer LS 50 B fluorimeter. The solution was stirred and temperature was maintained at 25 ± 1 °C. Following equilibration, the fluorescence of the tryptophan residues of the protein (λ_{ex} = 280 nm, λ_{em} = 340 nm) was followed as a function of time. When the fluorescence signal did not change with time (a stable baseline was reached), 100 μL of a solution of ethoxzolamide (K_d^{mono} = 0.2 nM in PBS at pH 7.4) was added to the stirred solution of $(CA)_2$ and ligand. The time immediately following the brief mixing period (~10 s) was taken as time zero (t = 0 s.). The fluorescence signal was normalized from time zero to the end of the experiment.

Determination of Avidities for the Binding of LRL to $(CA)_2$. To the wells of a black 96-microwell plate was added L or LRL (which was diluted serially across the 12 wells of the plate) followed by a solution of $(CA)_2$ (25 nM final concentration) in a final volume of 200 μL of 20 mM sodium phosphate pH 7.4. The covered plate was incubated at 25 °C for more than 2 h. The intensity of the fluorescence was measured about five times (λ_{ex} = 290 nm, λ_{em} = 460 nm, with a 455 nm cutoff filter). The intensities were fit to eq S21 (Supporting Information).

Crystallization of $(CA)_2$. Crystals were grown by vapor diffusion from a reservoir solution of 2.0 M ammonium sulfate at pH 8.8 (bicine). The crystals appeared as thin plates and grew to their full size (approximately 0.4 mm × 0.4 mm × 0.1 mm) in about 2 weeks at 4 °C. A crystal was captured in a nylon loop, transferred to a 20% glycerol/85% reservoir cryoprotectant solution briefly, rapidly frozen in a liquid nitrogen bath, and finally mounted in a cryostream (Oxford Cyrosystems). The X-ray source was a rotating copper anode, and diffraction data were collected on an RAXIS IV (Rigaku) instrument. The data set used in this structure was measured from a single crystal. The data describing these crystals appears in the Supporting Information (PDB 3PJJ).

Molecular Modeling. Models of $(CA)_2$ with bivalent ligands were prepared using the Molecular Operating Environment (MOE) program available from Chemical Computing Group, Inc. The models of the dimer−ligand complexes were constructed using the coordinates of the crystal structure of $(CA)_2$ and bivalents ligands constructed within MOE. Two Zn−N bonds were created between the sulfonamides of the ligands and the zinc atoms in the active sites of the dimer. The internal coordinates of the CA monomers were fixed, and the energy of the complex was minimized using the AMBER force field, allowing the bonds within bivalent ligand and the linker joining the monomers of CA to rotate. A pdb file of the structure with the minimum energy was saved and rendered in Pymol.

ASSOCIATED CONTENT

Supporting Information. Analytical ultracentrifugation experiments, derivation of eq S21, synthesis of $(CA)_2$, and collection

of X-ray data. This material is available free of charge via the Internet at http://pubs.acs.org.

AUTHOR INFORMATION

Corresponding Author
gwhitesides@gmwgroup.harvard.edu

ACKNOWLEDGMENT

This work was supported by the NIH through a research award (GM030367) and by the Wyss Institute for Biologically Inspired Engineering at Harvard. E.T.M. acknowledges the support of the NIH in the form of a postdoctoral fellowship (NRSA-GM076971). D.T.M. acknowledges support from an NIH postdoctoral fellowship (1 F32 AI068605-0). We thank Prof. Krishna Kumar (Tufts University) for his help with analytical ultracentrifugation experiments (NIH 1S10RR017948).

REFERENCES

(1) Murphy, K.; Travers, P.; Walport, M. *Janeway's Immunobiology*, 7 ed.; Garland Science, Taylor & Francis Group, LLC: New York, 2008.
(2) Houk, K. N.; Leach, A. G.; Kim, S. P.; Zhang, X. Y. *Angew. Chem., Int. Ed.* **2003**, *42*, 4872.
(3) Mack, E. T.; Snyder, P. W.; Perez-Castillejos, R.; Whitesides, G. M. *J. Am. Chem. Soc.* **2011**, *133*, 11701.
(4) Gestwicki, J. E.; Cairo, C. W.; Strong, L. E.; Oetjen, K. A.; Kiessling, L. L. *J. Am. Chem. Soc.* **2002**, *124*, 14922.
(5) Mourez, M.; Collier, R. J. *Use of Phage Display and Polyvalency to Design Inhibitors of Protein-Protein Interactions*; Humana Press Inc.: Totowa, NJ, 2004; Vol. 261.
(6) Ernst, B.; Magnani, J. L. *Nat. Rev. Drug Discovery* **2009**, *8*, 661.
(7) Vance, D.; Shah, M.; Joshi, A.; Kane, R. S. *Biotechnol. Bioeng.* **2008**, *101*, 429.
(8) Krishnamurthy, V. M.; Estroff, L. A.; Whitesides, G. M. In *Fragment-based Approaches in Drug Discovery*; Jahnke, W., Erlanson, D. A., Eds.; Wiley-VCH: Weinheim, 2006; Vol. 34.
(9) Schweitzer-Stenner, R.; Licht, A.; Luescher, I.; Pecht, I. *Biochemistry* **1987**, *26*, 3602.
(10) Das, R.; Diallo, M.; Baird, E.; Coates, G.; GoldStein, B.; Holowka, D.; Baird, B. *Biophys. J.* **2004**, *86*, 448A.
(11) Baird, B.; Posner, R.; Goldstein, B.; Holowka, D. *FASEB J.* **1991**, *5*, A652.
(12) Subramanian, K.; Holowka, D.; Baird, B.; Goldstein, B. *Biochemistry* **1996**, *35*, 5518.
(13) Das, R.; Baird, E.; Allen, S.; Baird, B.; Holowka, D.; Goldstein, B. *Biochemistry* **2007**, *47*, 1017.
(14) Bilgiçer, B.; Moustakas, D. T.; Whitesides, G. M. *J. Am. Chem. Soc.* **2007**, *129*, 3722.
(15) Mammen, M.; Choi, S.-K.; Whitesides, G. M. *Angew. Chem., Int. Ed.* **1998**, *37*, 2755.
(16) Burton, R. E.; Hunt, J. A.; Fierke, C. A.; Oas, T. G. *Protein Sci.* **2000**, *9*, 776.
(17) Christianson, D. W.; Fierke, C. A. *Acc. Chem. Res.* **1996**, *29*, 331.
(18) Krebs, J. F.; Ippolito, J. A.; Christianson, D. W.; Fierke, C. A. *J. Biol. Chem.* **1993**, *268*, 27458.
(19) Nair, S. K.; Calderone, T. L.; Christianson, D. W.; Fierke, C. A. *J. Biol. Chem.* **1991**, *266*, 17320.
(20) Supuran, C. T.; Scozzafava, A.; Casini, A. *Med. Res. Rev.* **2003**, *23*, 146.
(21) Krishnamurthy, V. M.; Kaufman, G. K.; Urbach, A. R.; Gitlin, I.; Gudiksen, K. L.; Weibel, D. B.; Whitesides, G. M. *Chem. Rev.* **2008**, *108*, 946.
(22) Krishnamurthy, V. M.; Semetey, V.; Bracher, P. J.; Shen, N.; Whitesides, G. M. *J. Am. Chem. Soc.* **2007**, *129*, 1312.
(23) Ercolani, G. *J. Am. Chem. Soc.* **2003**, *125*, 16097.
(24) Hunter, C. A.; Anderson, H. L. *Angew. Chem., Int. Ed.* **2009**, *48*, 7488.
(25) Sidido, M.; Kanazawa, Y.; Imanishi, Y. *Biopolymers* **1981**, *20*, 653.
(26) Krishnamurthy, V. M.; Bohall, B. R.; Semetey, V.; Whitesides, G. M. *J. Am. Chem. Soc.* **2006**, *128*, 5802.
(27) Ostuni, E.; Chapman, R. G.; Holmlin, R. E.; Takayama, S.; Whitesides, G. M. *Langmuir* **2001**, *17*, 5605.
(28) Mack, E.; Cummings, L.; Perez-Castillejos, R. *Anal. Bioanal. Chem.* **2011**, *399*, 1641.
(29) Lebowitz, J.; Lewis, M. S.; Schuck, P. *Protein Sci.* **2002**, *11*, 2067.
(30) Chen, R. F.; Kernohan, J. C. *J. Biol. Chem.* **1967**, *242*, 5813.
(31) Dembo, M.; Goldstein, B. *J. Immunol.* **1978**, *121*, 345.
(32) Lundquist, J. J.; Toone, E. J. *Chem. Rev.* **2002**, *102*, 555.
(33) Wiseman, T.; Williston, S.; Brandts, J. F.; Lin, L.-N. *Anal. Biochem.* **1989**, *179*, 131.
(34) Mecinovic, J.; Snyder, P. W.; Mirica, K. A.; Bai, S.; Mack, E. T.; Kwant, R. L.; Moustakas, D. T.; Heroux, A.; Whitesides, G. M. *J. Am. Chem. Soc.* **2011**, *133*, 14017–14026.
(35) Kramer, R. H.; Karpen, J. W. *Nature* **1998**, *395*, 710.
(36) Chan, W. C.; White, P. D. *Fmoc solid phase peptide synthesis a practical approach*; Oxford University Press: New York, 2000.